energies

MDPI

Article

Simulation Research on Regenerative Braking Control Strategy of Hybrid Electric Vehicle

Cong Geng, Dawen Ning *, Linfu Guo, Qicheng Xue and Shujian Mei

Beijing Key Laboratory of Powertrain Technology for New Energy Vehicles, Beijing Jiaotong University, Beijing 100044, China; cgeng@bjtu.edu.cn (C.G.); lfguo@bjtu.edu.cn (L.G.); 17116356@bjtu.edu.cn (Q.X.); 20121390@bjtu.edu.cn (S.M.)

* Correspondence: 18121397@bjtu.edu.cn

Abstract: This paper proposes a double layered multi parameters braking energy recovery control strategy for Hybrid Electric Vehicle, which can combine the mechanical brake system with the motor brake system in the braking process to achieve higher energy utilization efficiency and at the same time ensure that the vehicle has sufficient braking performance and safety performance. The first layer of the control strategy proposed in this paper aims to improve the braking force distribution coefficient of the front axle. On the basis of following the principle of braking force distribution, the braking force of the front axle and the rear axle is reasonably distributed according to the braking strength. The second layer is to obtain the proportional coefficient of regenerative braking, considering the influence of vehicle speed, braking strength, and power battery state of charge (*SOC*) on the front axle mechanical braking force and motor braking force distribution, and a three-input single-output fuzzy controller is designed to realize the coordinated control of mechanical braking force and motor braking force of the front axle. Finally, the AMESim and Matlab/Simulink co-simulation model was built; the braking energy recovery control strategy proposed in this paper was simulated and analyzed based on standard cycle conditions (the NEDC and WLTC), and the simulation results were compared with regenerative braking control strategies A and B. The research results show that the braking energy recovery rate of the proposed control strategy is respectively 2.42%, 18.08% and 2.56%, 16.91% higher than that of the control strategies A and B, which significantly improves the energy recovery efficiency of the vehicle.

Keywords: hybrid electric vehicle; energy recovery; braking strength; control strategy

Citation: Geng, C.; Ning, D.; Guo, L.; Xue, Q.; Mei, S. Simulation Research on Regenerative Braking Control Strategy of Hybrid Electric Vehicle. *Energies* **2021**, *14*, 2202. https://doi.org/10.3390/en14082202

Academic Editor: Luis Vaccaro

Received: 8 March 2021
Accepted: 10 April 2021
Published: 15 April 2021

1. Introduction

Since hybrid electric vehicles (HEV) are equipped with a motor drive system that can not only select the appropriate driving mode according to the current driving conditions, but can also recover energy during braking, thus improving energy utilization efficiency and reducing exhaust gas pollution, which has gradually become a major development trend in the automobile industry [1]. Among them, braking energy recovery technology is one of the core technologies of hybrid electric vehicles. It can convert the kinetic energy generated during braking into electrical energy and store it in the energy storage device to stop it from turning into heat energy and dissipating in the air [2,3]. However, in the process of vehicle braking energy recovery, considering the influence of factors such as braking safety, overcharging of energy storage devices and energy recovery efficiency, the braking force provided by the motor is limited and cannot meet the braking requirements of the vehicle. At this time, in order to ensure that the vehicle can brake smoothly, the mechanical braking force and the motor braking force need to work together [4,5]. Therefore, the coordinated control between the mechanical braking force and the motor braking force occupies an important position in the development of braking energy recovery technology.

At present, the research into braking energy recovery technology mainly aims at improving the efficiency of vehicle braking energy recovery to distribute the braking

force reasonably. The literature [6] identifies the driver's driving intention according to the opening degree and change rate of the brake pedal, so that the motor can provide appropriate regenerative braking torque to meet the driver's braking requirements and reduce the driving burden. In the literature [7], the torque distribution between mechanical braking force and motor braking force has been studied, and a series of regenerative braking control strategies have been proposed. These strategies are based on the motor power limitation and the driver's braking requirements, so that the vehicle's regenerative braking force is always at the highest critical value to ensure efficient braking efficiency. In the literature [8], maximum energy recovery is aimed for, and the influence of motor speed and battery *SOC* on regenerative braking is considered, distributing the braking force of the front and rear axles and the electromechanical braking force of the vehicle. In the literature [9], a fuzzy controller with a battery *SOC* and braking strength as variables for rear-drive hybrid electric vehicles have been designed, which has realized the coordinated control of the mechanical brake system and the motor brake system, and has achieved the purpose of energy recovery. In [10], in order to solve the adverse effect of the current on the battery during the regenerative braking of the vehicle, a regenerative braking control strategy is proposed. This strategy optimizes the distribution of electromechanical braking force according to the optimal slip rate of the vehicle, reducing battery capacity loss while maximizing braking energy. In [11], a new braking torque distribution control strategy to maximize the energy recovery of the regenerative braking system, and optimize the braking torque distribution of the front and rear axles while ensuring braking safety was designed, further improving the recovery of vehicle braking energy.

The above research mainly focuses on the coordinated control of the mechanical-motor composite braking system in the process of vehicle braking to realize the distribution of mechanical braking force and motor braking force. However, the factors affecting energy recovery were not comprehensive in the above studies, and the comparison of various braking energy recovery control strategies was not carried out, which could not directly prove the effectiveness of the strategy. Therefore, in order to ensure the vehicle's stable braking performance and efficient energy recovery, this paper proposes a double layered multi parameters braking energy recovery control strategy. This strategy takes into account the influences of engine anti-drag torque, vehicle speed, braking strength and power battery *SOC* on the hierarchical control of vehicle braking force distribution, and compares it with other braking force distribution control strategies.

This paper is organized as follows: In Section 2, the main components of the vehicle's braking system are analyzed, and the main framework of the control strategy in this paper is given; in Section 3, with the goal of increasing the front axle braking force distribution coefficient, different braking modes are formulated according to the braking strength, and the front and rear axle braking forces are distributed for each mode; in Section 4, based on the designed multi parameters fuzzy controller, the front axle braking force obtained from the upper layer is secondarily distributed to realize the coordinated control of the electromechanical braking force of the front axle; in Section 5, the strategy is co-simulated and analyzed by AMESim and Matlab/Simulink software, and the control strategy proposed in this paper is compared with other "braking strength-fuzzy" control strategies to verify the energy recovery effect of the control strategy proposed in paper; finally, Section 6 presents the conclusions of this study.

2. System Analysis and Modelling

2.1. Structure of Braking Energy Recovery System

In this paper, a hybrid electric vehicle is taken as the research object. The vehicle consists of driving wheel, main reducer, gear box, motor, power battery, DC/AC, converter, controller and energy management system in the process of braking energy recovery, as shown in Figure 1.

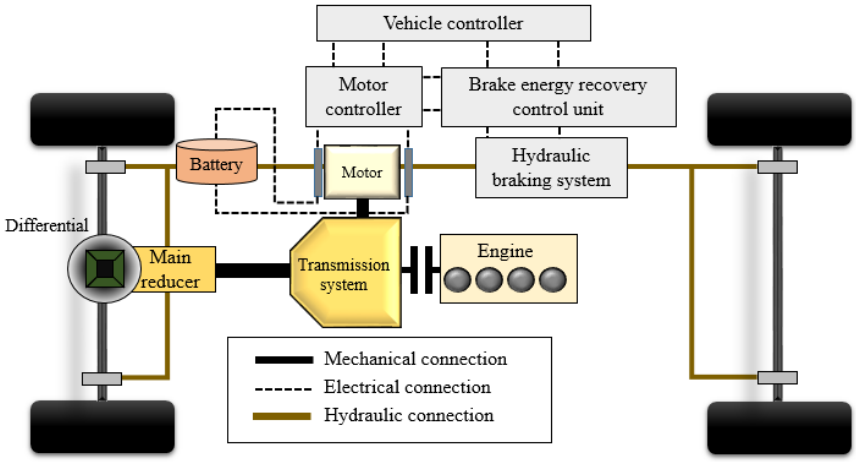

Figure 1. Schematic diagram of Hybrid Electric Vehicle.

When the vehicle is in the driving state, the engine and the motor are selected as the power source. When the vehicle is in the braking state, the brake signal obtained according to the position sensor on the brake pedal is transmitted to the vehicle controller to calculate the total required braking force. The total braking force is distributed by the braking energy recovery control unit between the front and rear axles and between the mechanical and motor braking forces. Then the motor provides the required regenerative braking torque, and part of the kinetic energy generated by braking is converted into electrical energy and stored in the power battery. During braking, the dynamic equation for a hybrid car is Equation (1).

$$\Sigma F = F_f + F_w + F_i + F_b \tag{1}$$

where, F is longitudinal force, F_w is air resistance force, F_f is rolling resistance, F_i is slope resistance force, F_b is the ground braking force.

2.2. Motor Model

When a hybrid car brakes, the motor acts as a generator for energy recovery. The working characteristics of a motor are closely related to its generating power. When the motor speed is less than the rated speed, the motor is in the constant torque range; when the motor speed is more than the rated speed, the motor is in the constant power range. The relationship between motor speed, torque and power is shown in Equation (2):

$$T = \begin{cases} T_n & n < n_0 \\ \frac{9550 P_n}{n} & n < n_0 \end{cases} \tag{2}$$

where T is the motor torque, T_n is the motor rated torque, n_0 is the motor rated speed and P_n is the motor rated power.

In the braking energy recovery control strategy, the external characteristic curve of motor braking is shown as Figure 2, and can be described as a one-dimensional table. By looking up the current motor speed in the table, the maximum torque is obtained.

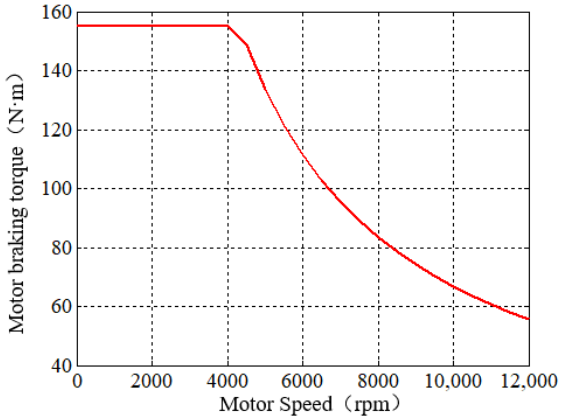

Figure 2. External characteristic curve of motor braking.

2.3. Power Battery Model

During the vehicle braking energy recovery process, the motor will restore the recovered energy in the power battery. When the *SOC* of the power battery is too high, to avoid damage to the battery, the braking energy will not be recovered.

In the process of braking energy recovery, the current open circuit voltage and the internal resistance of charging and discharging are obtained according to the current power battery *SOC* table to calculate the power battery's voltage and maximum charging and discharging power [12].

The *SOC* of the power battery is calculated by the ampere-hour integral method, as shown in Equation (3):

$$SOC = SOC_n - \frac{\int \eta I dt}{Q_n} \tag{3}$$

where SOC_n is the current moment Power Battery *SOC* value, Q_n is the power battery storage, I is power battery charge and discharge current, and η is the power battery charge, discharge efficiency value.

2.4. Engine Model

As one of the driving sources of hybrid electric vehicles, the engine converts the heat energy produced by combustion of fuel and other chemicals in the cylinder into mechanical energy to drive the vehicle forward. In the braking process, the engine stops the fuel supply or changes to an idling state. The vehicle drives the engine to operate compulsively to achieve the anti-drag braking torque.

Figures 3 and 4 show the external characteristic curves of the engine described by the relationship between engine speed and full-load driving and braking torque.

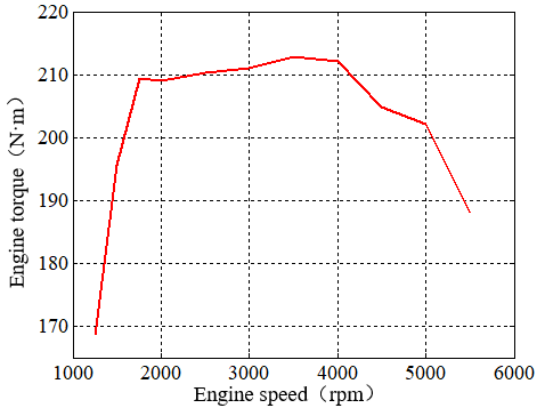

Figure 3. External characteristic curve of engine driving torque.

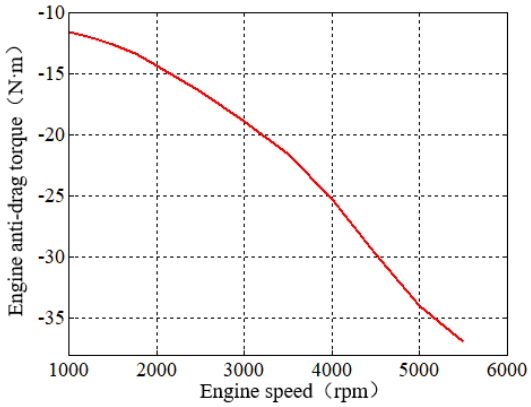

Figure 4. Engine speed and anti-drag torque diagram.

2.5. Vehicle Parameters

The hybrid electric vehicle parameters are shown in Table 1 (these parameters are provided by Chery Automobile Company):

Table 1. Vehicle parameters.

	Parameters	Numerical Value
Vehicle parameters	Windward area (m^2)	2.638
	Wheelbase (m)	2.710
	Vehicle fit-up quality (kg)	1545
	Rolling radius of tire (m)	0.347
	Height center of mass (m)	0.650
	Drive Mode (FWD/AWD/RWD)	FWD (front drive)
	Transmission ratio	3.12
Motor parameters	Maximum Motor Power (kw)	70
	Maximum torque of motor (N·m)	155
	Maximum speed of motor (rpm)	12,000
Battery parameter	Battery capacity (Ah)	75
	Voltage Range (V)	260~420

2.6. Braking Energy Recovery Control Strategy

The logic of the braking energy recovery control strategy established in this paper is shown in Figure 5.

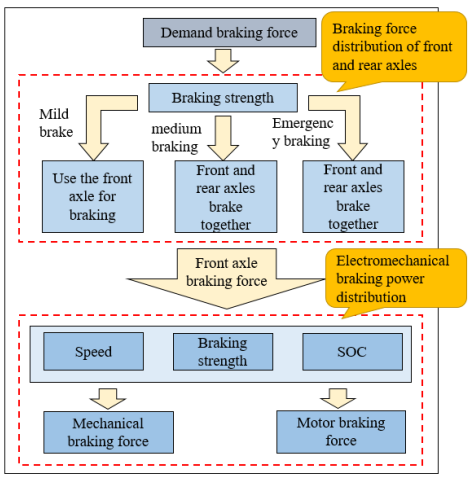

Figure 5. Logic diagram of braking energy recovery control strategy.

The braking energy recovery control strategy proposed in this paper is divided into two layers: front/rear braking force distribution and mechanical/motor braking force distribution. Firstly, three braking modes are determined according to the braking strength, mild braking, medium braking and emergency braking. Then, to ensure that the braking force is in the safe condition, the distribution of the braking force of the front and rear axles is made according to the current braking mode. This layer is the control strategy of front and rear axle braking force distribution. After the distribution of the front axle braking force, the fuzzy controller is designed to distribute the front axle mechanical braking force and the motor braking force, considering the influence of three factors: vehicle speed, braking strength and power battery *SOC*. This layer is the control strategy of the front axle electromechanical braking force.

3. Control Strategy of Braking Force Distribution for Front and Rear Axles

3.1. Relationship between Braking Strength and Braking Force Distribution Coefficient

In this paper, we studied the front-drive hybrid electric vehicle, so the braking force should be properly distributed to the front wheel. In the case of passenger cars, the ECE-R13 braking regulations clearly require the distribution of braking force between the front and rear axles [13]:

1. The braking strength should satisfy $z \geq 0.1 + 0.85(\varphi - 0.2)$ for the biaxial vehicle with an adhesion coefficient of 0.2~0.8;
2. when the braking strength z is 0.15~0.80, the adhesion coefficient utilization curve of the front axle should be above the adhesion coefficient utilization curve of the rear axle under various loads;
3. when the braking strength z is 0.30~0.45, if the adhesion coefficient utilization curve of the rear axle does not exceed 0.05 above the straight line determined by the formula $\varphi = z$, the adhesion coefficient utilization curve of the rear axle can be above the adhesion coefficient utilization curve of the front axle.

According to the above regulations, the braking force distribution coefficient is:

$$\begin{cases} \beta \leq \frac{(z+0.07)\left(b+zh_g\right)}{0.85zL} \; 0.1 \leq z \leq 0.61 \\ \beta \geq 1 - \frac{(z+0.07)\left(a-zh_g\right)}{0.85zL} \; 0.1 \leq z \leq 0.61 \\ \beta \geq \frac{b+zh_g}{L} \; 0.15 \leq z \leq 0.8 \end{cases} \tag{4}$$

where h_g is the height of the center of mass of the vehicle, L is the wheelbase of the vehicle, a is the distance from the front axle to the center of mass of the vehicle, and b is the distance from the rear axle to the center of mass of the vehicle.

The A line in Figure 6 is the upper boundary line of the braking force distribution coefficient β, and the β only satisfies the requirements of the braking regulations when the front axle uses the adhesion coefficient below the A line. The B line is the lower boundary line of the β, only when the β is above the B line, the rear axle can use the adhesion coefficient to meet the requirements of the law, and the C line is the sequence control line of the front and rear wheel locking, when the β is above the C line, the front wheel can be locked before the rear wheel locking, to prevent the rear wheel from throwing tail. As can be seen from the diagram, when the braking strength $z \leq 0.1$, there is no obvious restriction on the distribution of braking force in the regulations. The braking force can completely be supplied by the front axle, which means the braking force distribution coefficient β is 1. Therefore, if the value of β is between the A line and C line, it can meet the requirements of braking regulations and achieve vehicle braking stability.

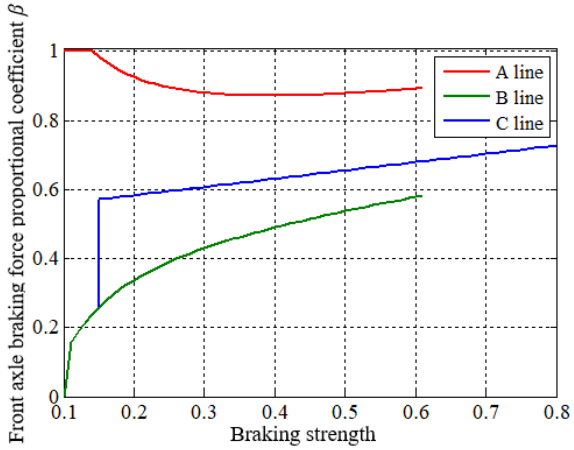

Figure 6. Relationship curve between braking force distribution coefficient and braking strength.

3.2. Braking Mode Division and Braking Force Distribution

According to the distribution range restricted by ECE-R13 braking regulations, the ideal braking distribution I curve and F group line [14], combined with the advantages of a traditional ideal braking distribution method, parallel braking force distribution method and maximum energy recovery distribution method, a braking force distribution control strategy for front and rear axles based on braking strength is proposed.

The braking force distribution control rules used in the front and rear axle braking force distribution control strategy based on braking strength are as shown in the curve ABCDEF in Figure 7. The braking force distribution of the front and rear axles according to the curve can not only ensure the braking safety of the vehicle in different braking strengths, but also increase the proportion of the braking force distribution of the front axles, so as to improve the recovery of the braking energy.

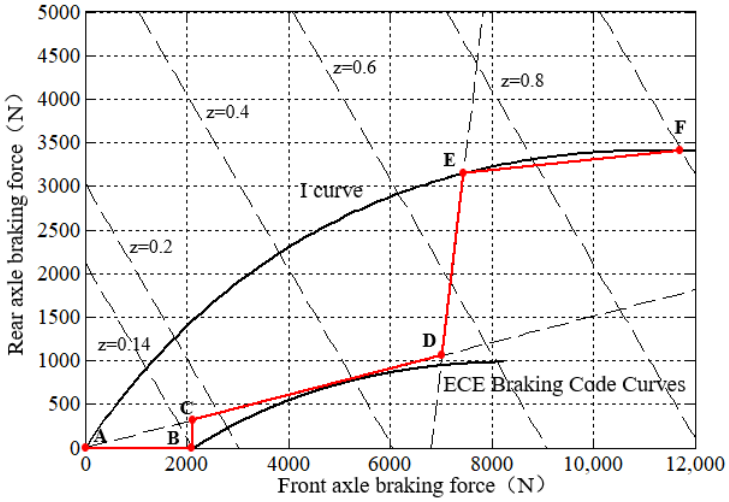

Figure 7. Front and rear axle braking force distribution curve.

The strategy divides the braking modes into three types: mild braking, moderate braking and emergency braking, in which the medium braking consists of two curves. The front and rear axle braking forces for each mode of braking will be distributed according to the following principles:

(1) When the braking strength $z \leq 0.14$, the vehicle is in the mild braking stage, and the braking force of the front and rear axles is distributed according to the line AB. In this case, since the braking force needed by the vehicle is small, the braking can be completed only with the front axle.

Therefore, the braking force distribution coefficient $\beta = 1$, and the front and rear axle braking force distribution control strategy is:

$$\begin{cases} F_{bf} = Gz \\ F_{br} = 0 \end{cases} \tag{5}$$

where F_{bf} is the front axle braking force; F_{br} is the rear axle braking force, and G is the hybrid electric vehicle gravity.

(2) When the braking strength is $0.14 < z \leq 0.53$, the vehicle is in the moderate braking stage and the braking force of the front and rear axles is distributed according to the BC and CD line. At this time, the mechanical braking force and the motor braking force work together. In order to recover the energy better, the braking force should be distributed to the front axles as much as possible within a reasonable range. Because the ECE braking regulation curve presents a non-linear braking force distribution law, which may make the whole system design more complicated. In order to make the calculation of the front and rear axle braking force distribution control strategy more convenient, a linear curve, CD (through the origin and tangent to the ECE curve), is used to replace the ECE curve. In the BC curve, with the increase in braking strength, the braking force of the front axle remains unchanged, while the braking force of the rear axle gradually increases until it is connected with CD.

The front axle braking force distribution coefficient β of the CD segment is obtained by taking a derivative of the Formula (4) $\beta = \frac{(z+0.07)\left(b+zh_g\right)}{0.85Lz}$ and replacing the calculated value with Z in the equation to obtain the front axle braking force distribution coefficient β of segment CD, as shown in Equation (6).

$$\beta = \frac{2\sqrt{0.07b/h_g} + b + 0.07h_g}{0.85L} \tag{6}$$

where b is the distance between the rear axle and the vehicle center of mass, h_g is the height of the vehicle center of mass, L is the vehicle wheelbase.

Taking the parameters into Equation (6), we get $\beta = 0.8722$. The distribution control strategy for the front and rear axles is:

$$\begin{cases} F_{bf} = \frac{(1-0.8722)}{0.8722} F_{br} \\ F_{br} = Gz - F_{bf} \end{cases} \tag{7}$$

(3) When the braking strength is $0.53 < z \leq 0.7$, the vehicle is in the moderate braking stage, the braking force is distributed according to DE line (F group line). As the braking strength gradually increases, the proportion of the braking force of the rear axle gradually increases. The braking mode gradually transitions from moderate braking to emergency braking.

At this point, the front axle braking force distribution coefficient β ranges from (0.7030, 0.8722), and the front and rear axle braking force distribution control strategies are:

$$\begin{cases} F_{br} = \frac{L-\varphi h_g}{\varphi h_g} F_{bf} - \frac{Gb}{h_g} \\ F_{bf} = Gz - F_{br} \end{cases} \tag{8}$$

where φ is the road surface adhesion coefficient, chosen to be 0.7 in this paper.

(4) When the braking strength $z > 0.7$, the vehicle is in the emergency braking stage, and only the mechanical braking force is involved in the braking. In order to make the vehicle brake safely, it is the best choice to hold the front and rear wheels together along the ideal I curve, but it is difficult to meet this condition in reality, so the distribution curve should be as close to the I curve as possible. Therefore, the front and rear axle braking forces are distributed according to the EF line.

At this point, the front axle braking force distribution coefficient β ranges from (0.7030, 0.7749). The braking force distribution strategy for the front and rear axles is as follows:

$$\begin{cases} F_{br} = 0.0607F_{bf} + 2696.3 \\ F_{bf} = Gz - F_{br} \end{cases} \quad (9)$$

4. Control Strategy of Electromechanical Braking Force Distribution for Front Axle

Fuzzy control is the use of fuzzy mathematics, combined with practical engineering experience of the control theory and method [15]. Since this paper is aimed at the front-drive hybrid electric vehicle, it is necessary to redistribute the front-axle braking force calculated in the previous content to get the front-axle mechanical braking force and motor braking force (regenerative braking force); however, the process of electromechanical braking force distribution is affected by many factors, and there is no clear mathematical model between each factor and regenerative braking force distribution, so fuzzy rule control is the most ideal method.

In this paper, three parameters of real-time vehicle speed, braking strength and power battery *SOC* are taken as input, and the proportional coefficient of regenerative braking K is taken as the output to build a fuzzy controller. By adding the established fuzzy controller to the braking force distribution strategy mentioned above, the braking force distribution between the front and rear axles and between the mechanical and motor braking force of the front axles can be realized. Figure 8 is the structure diagram of the established electromechanical braking force distribution strategy.

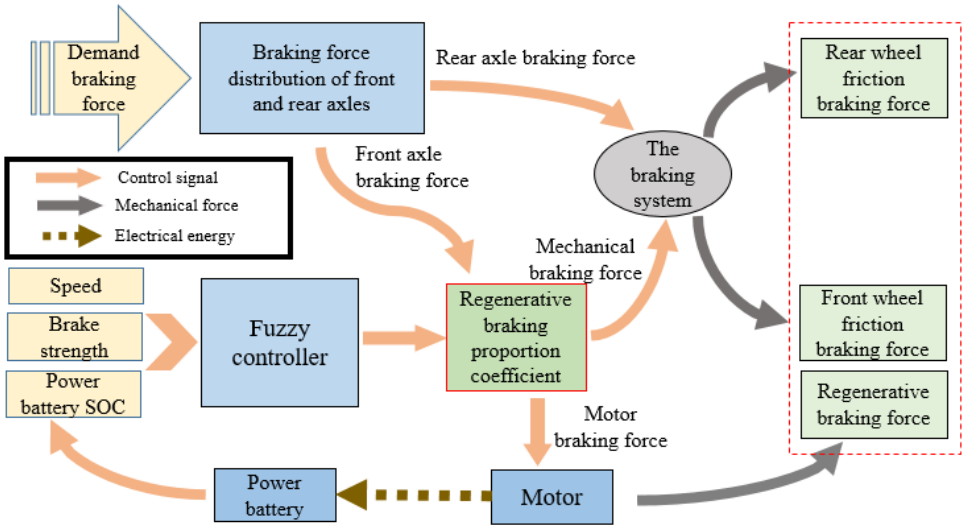

Figure 8. Electromechanical braking force distribution fuzzy control structure.

4.1. Design of Fuzzy Controller

Firstly, the input variable and the output variable are fuzzified, that is, the membership function of each variable is determined. In this paper, the fuzzy reasoning system is established by using MATLAB, and the membership function of input variable and output variable is designed, in which the trapezium (TRAPMF) type is used as the input, and the two-sided trapezium type and the middle triangle (TRIMF) type are used as the output.

In this system, the membership function of the input variable v is divided into three fuzzy subsets: {L, M, H}, the fuzzy language variable is described as L (low), M (middle), H (high), and the fuzzy universe is (0,120); the membership function of braking strength z is divided into three fuzzy subsets: {L, M, H}, the fuzzy language variable is described as L (low), M (middle), H (high), and the fuzzy universe is [0,1], the membership function of power battery *SOC* is divided into three fuzzy subsets: {L, M, H}, the fuzzy language variables are described as L (low), M (middle), H (high) and the fuzzy universe is (0,1). The

membership function of the output variable regenerative braking proportional coefficient K is divided into five fuzzy subsets: {LL, L, M, H, HH}, whose fuzzy language variables are described as VL (very low), L (low), M (medium), H (high), VH (very high) and the fuzzy universe is (0,1). The membership function of the input and output variables is shown in Figure 9.

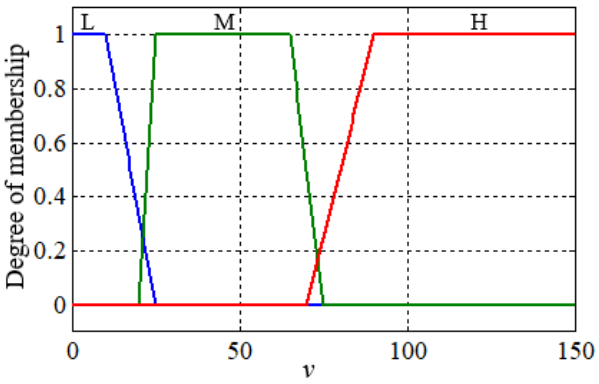

(**a**) The membership function of velocity v

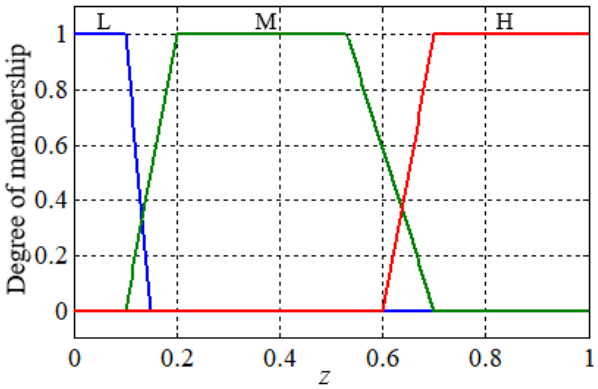

(**b**) The membership function of braking strength z

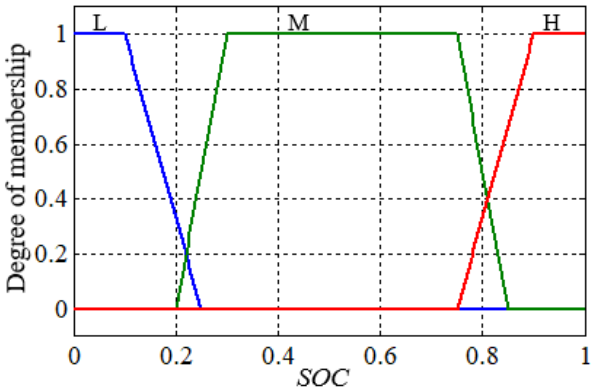

(**c**)The membership function of Power Battery SOC

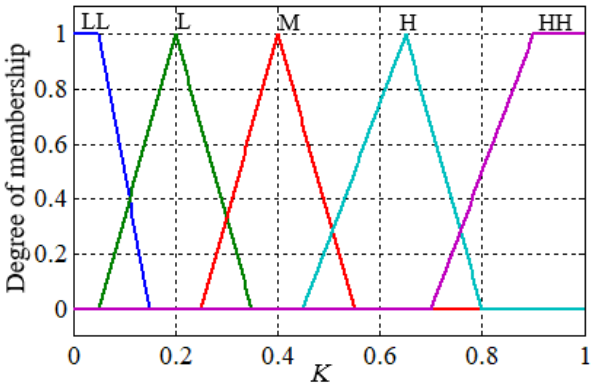

(**d**) The membership function of the proportional coefficient K of regenerative braking

Figure 9. Input and output variable membership functions.

4.2. Fuzzy Rules

Fuzzy rules are realized by the combination of fuzzy languages, which is based on a great deal of practical engineering experience [16]. In this paper, the braking stability and the service life of the power battery of the vehicle in the process of regenerative braking force distribution of the front axle are comprehensively considered. Using the IF-THEN logic rule to design the fuzzy rules, a rule is expressed as follows:

$$if\ v\ is\ v_i,\ and\ SOC\ is\ SOC_i\ ,\ and\ z\ is\ z_i\ ;then\ K\ is\ K_i.$$

The fuzzy rules table is shown in Table 2 below.

MATLAB is used to establish Table 2 fuzzy rules in a three-dimensional graph, as shown in Figure 10. As shown in Figure 10, when the v is high, the K is close to 1, and motor braking force is mainly used to recover the energy, but when v is too low, because the energy generated by the vehicle is low, mechanical braking is mainly used; when the SOC of power battery is high, the K is decreased and the energy recovery is reduced to avoid the effect of overcharge on the battery life. Therefore, K is proportional to v and inversely proportional to z and SOC of the power battery.

Table 2. Fuzzy rule table.

	V	*SOC*	*z*	*K*		*v*	*SOC*	*z*	*K*
1	L	H	L	VL	15	M	M	H	VL
2	L	H	M	VL	16	H	M	L	VH
3	L	H	H	VL	17	H	M	M	H
4	M	H	L	VL	18	H	M	H	VL
5	M	H	M	VL	19	L	L	L	M
6	M	H	H	VL	20	L	L	M	M
7	H	H	L	VL	21	L	L	H	VL
8	H	H	M	VL	22	M	L	L	H
9	H	H	H	VL	23	M	L	M	H
10	L	M	L	L	24	M	L	H	VL
11	L	M	M	M	25	H	L	L	VH
12	L	M	H	VL	26	H	L	M	H
13	M	M	L	VH	27	H	L	H	VL
14	M	M	M	VH					

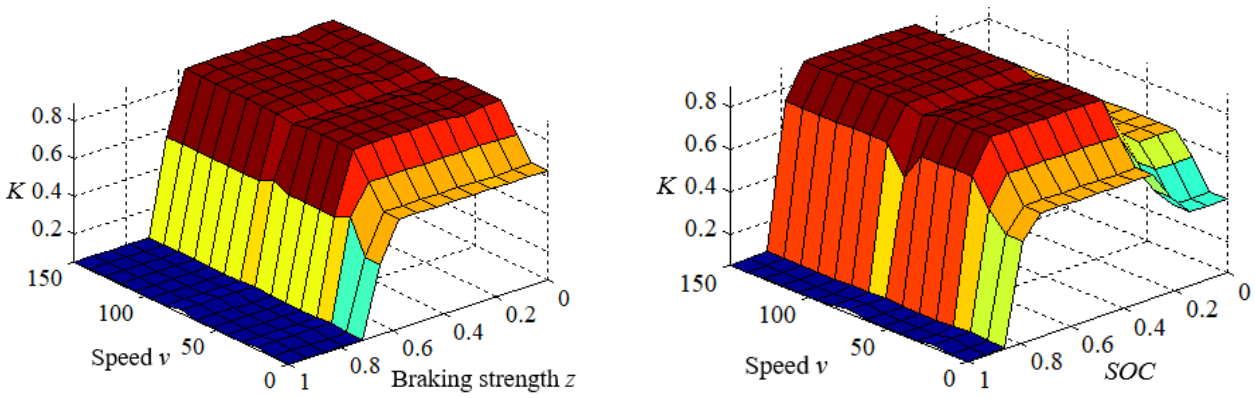

(**a**) *K* and Speed *v*, Braking strength *z* Change Relation Plot (**b**) *K* and Speed *v*, Power Battery *SOC* Change Relation Plot

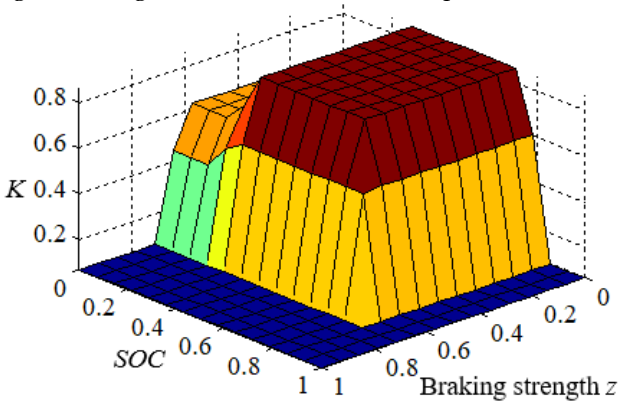

(**c**) *K* and Braking strength *z*, Power Battery *SOC*, Change Relation Plot

Figure 10. Fuzzy relation between inputs and *K*.

4.3. Defuzzification

Finally, the centroid method is used to defuzzify, and after calculation, the effective value of the proportional coefficient *K* of the regenerative braking is finally obtained. In this paper, the formula of the centroid method is as follows:

$$K = \frac{\sum_{i=1}^{n} \lambda_i k_i}{\sum_{i=1}^{n} \lambda_i} \tag{10}$$

where λ_i is the application of rule I calculated results; n is the number of fuzzy rules; k_i is the calculated proportion of the output by the application of rule i; and K is the system output accuracy.

5. Simulation Results and Analysis

5.1. Simulation Analysis of Braking Energy Recovery Control Strategy for Hybrid Electric Vehicle

This paper chooses AMESim and MATLAB/Simulink software to carry on the joint simulation, and AMESim simulation platform mainly aims at the structure modeling of hybrid electric vehicle, including driver model, motor model, vehicle model, battery model, transmission model, etc. While the MATLAB/Simulink simulation platform mainly aims at the establishment of a braking energy recovery control strategy model.

Using NEDC (New European Driving) and WLTC (Worldwide harmonized light vehicles test procedure) conditions [17], the double layers multi parameters braking energy recovery control strategy proposed in this paper was simulated and tested, setting the initial value of the vehicle power battery *SOC* to 0.5.

(1) NEDC condition

The NEDC condition is shown in Figure 11 below.

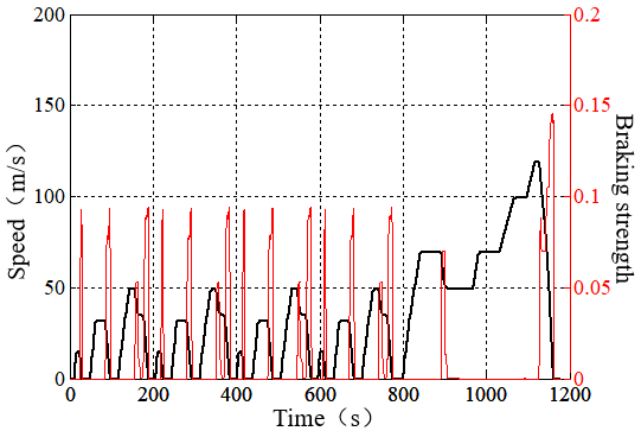

Figure 11. Working condition of NEDC.

NEDC condition is an organic combination of ECE road mode and suburban cycle mode [18], which can reflect the road conditions of urban and suburban roads steadily and accurately. Because the hybrid electric vehicle is driven by the dual power source of engine and motor, the anti-drag force generated by the engine must be subtracted before the braking force is distributed. Figures 12 and 13 both show the torque-time variation of the vehicle in the braking energy recovery control strategy proposed in this paper, in which Figure 12a shows the distribution of the mechanical braking torque between the front and rear axles and the braking torque distribution between the mechanical and motor of the front axle. In the first 800 s, in the urban condition, the vehicle mainly relies on the front axle in braking. Therefore, at this stage, the mechanical braking torque of the vehicle front axle is about 280 N·m, while the motor braking torque changes with the vehicle speed. When the vehicle speed is low, the motor braking torque is about 60 N·m; when the speed is high, the motor braking torque is about 110 N·m; between 800 s and 1180 s, the vehicle is in the suburban condition. As can be seen from Figure 12b, the front and rear axles of the vehicle participate in braking together during the period from 1154 s to 1159 s, the mechanical braking torque of the front axle reaches the maximum value of 450 N·m, and the rear axle braking torque is about 100 N·m. The motor braking torque first rises to its maximum value of 155 N·m and then drops to about 85 N·m.

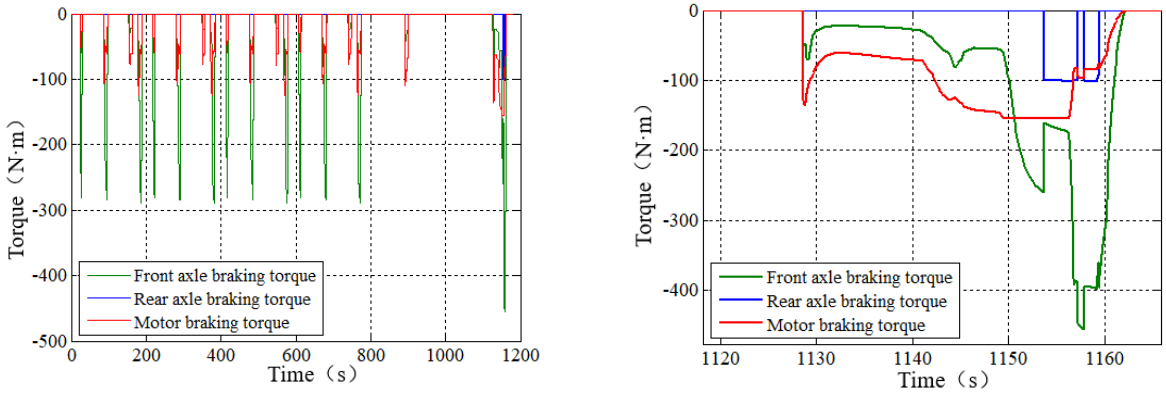

(**a**) Torque at NEDC condition (**b**) Local magnification of torque distribution

Figure 12. Vehicle braking torque distribution in the NEDC condition.

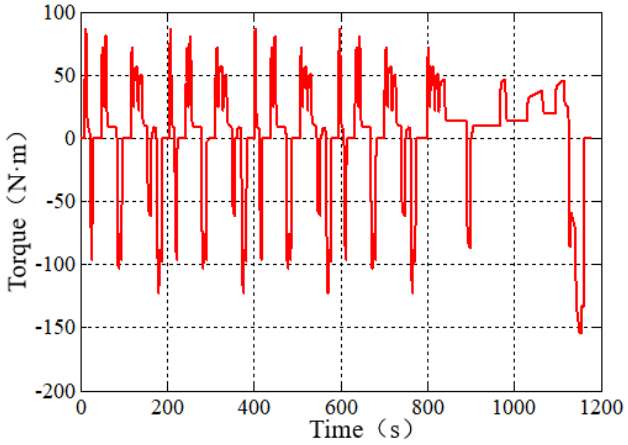

Figure 13. Motor torque in the NEDC condition.

The motor torque of the vehicle in the entire NEDC condition is shown in Figure 13. When the motor torque is positive, it means the vehicle is in the state of discharging driving, and when the motor torque is negative, it means the vehicle is in the state of charging. When the vehicle is in an urban condition, the changes of motor charge and discharge are frequent because of more vehicle start–stop times, and the changes of motor charge and discharge are less when the vehicle is in the suburban condition.

Figure 14 shows the anti-drag torque of the hybrid electric vehicle engine in the NEDC condition. During the braking process of the vehicle, the engine is in an idling state and will be forced to run by the vehicle. At this time, the engine will provide a part of the braking torque.

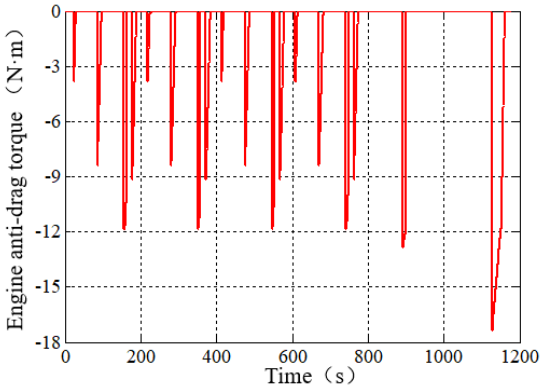

Figure 14. Engine anti-drag torque in the NEDC condition.

(2) WLTC condition

The WLTC condition is shown in Figure 15 below. It can be seen from the figure that in the WLTC condition, the vehicle speed fluctuates greatly, idling conditions are less, and there is no special regularity; it covers a wider speed range and the test cycle is longer.

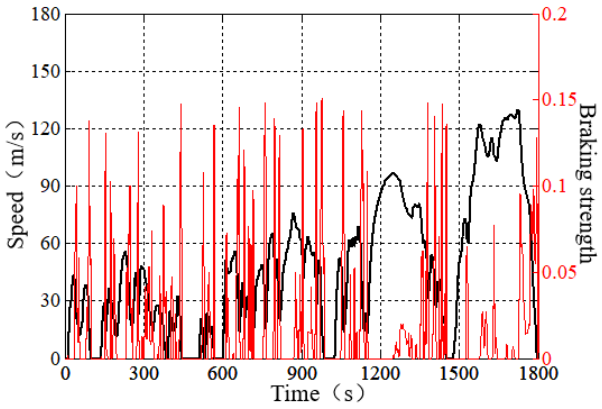

Figure 15. Working condition of WLTC.

Figure 16 shows the braking torque distribution of the hybrid electric vehicle in the WLTC condition. It can be seen from the figure that in this working condition, the vehicle starts and stops frequently and the braking strength is low. It mainly relies on the front axle brake for braking, and the motor braking torque is basically at a peak state, the rear axle brake participates in the braking work less frequently. During the entire braking process, the front axle mechanical braking torque is mainly between 220–280 N·m, and the motor braking torque is maintained at about 155 N·m.

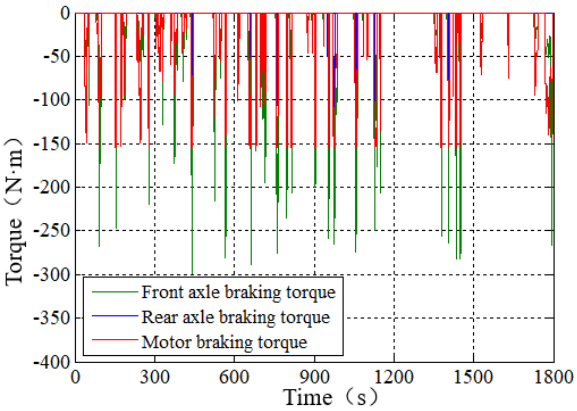

Figure 16. Vehicle braking torque distribution in the WLTC condition.

Figures 17 and 18 show the motor torque of the hybrid electric vehicle and the engine anti-drag torque during braking. From Figure 17, it can be seen that in this driving condition, the motor torque fluctuates greatly, and the motor braking torque remains at the peak state for a long time. It can be seen from Figure 18 that the engine anti-drag torque has been around 12.5 N·m for a long time.

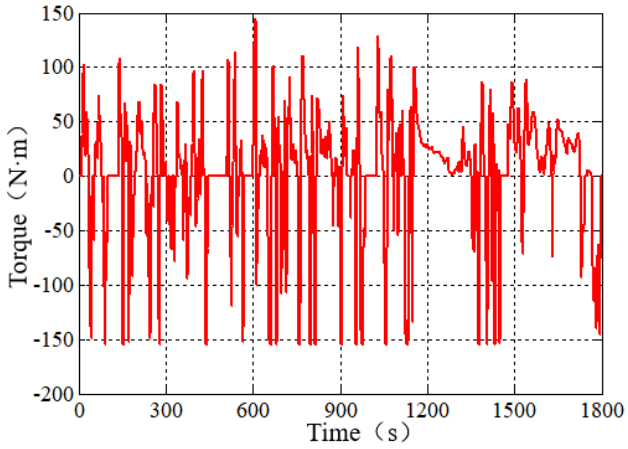

Figure 17. Motor torque in the NEDC condition.

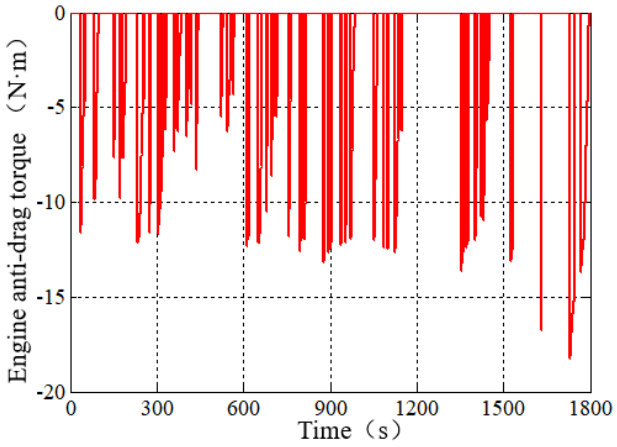

Figure 18. Engine anti-drag torque in the WLTC condition.

5.2. Comparative Analysis of Simulation Results of Different Braking Energy Recovery Control Strategies

In this paper, two braking energy recovery control strategies, A and B, were selected as the contrast, the simulation results of the control strategy proposed in this paper were compared with them. The *SOC* of power battery and energy recovery rate were taken as the evaluation indexes to verify the control strategy.

Control Strategy A: When the vehicle is in mild braking, only the front axle brake is used for braking; on the contrary, the braking force distribution of the front and rear axles is carried out along the ideal braking curve. When the braking force distribution of the front axle is carried out, the fuzzy control adopts the same method as this paper. Control Strategy B: Front and rear axle braking force distribution control strategy is the same as this paper, and the front axle electromechanical braking force distribution is distributed according to a fixed coefficient, that is, the superimposed control strategy. At present, the mechanical braking system of most hybrid electric vehicles cannot be decoupled, and the distribution coefficient between the regenerative braking force and the mechanical braking force cannot be changed at will [19]. Therefore, they all use a superposition control strategy, which has a low cost and a simple structure, but a limited energy recovery.

(1) NEDC condition

Since the motor braking torque is positively correlated with the recovered braking energy, the magnitude of the motor braking torque can directly indicate the effect of energy recovery of the vehicle braking system. Figure 19a is the comparison of motor braking torque of three control strategies. From the figure, it can be seen that the motor braking

torque of the control strategy proposed in this paper is superior to the control strategies A and B, proving that compared with the control strategies A and B, the control strategy proposed in this paper has some advantages in braking energy recovery. The decline curve of *SOC* of power battery represents the vehicle energy consumption. If the *SOC* curve of the power battery decreases slowly, it means that the power battery energy consumption is low while the vehicle is running in this condition. From Figure 19b, it can be seen that the initial *SOC* value of the three control strategies is 50%. At the end of the simulation, the *SOC* values of the three control strategies are 47.65%, 47.55% and 47.22% respectively. Because the NEDC condition is 11.03 km, when the vehicle drives 100 km, the battery *SOC* of the control strategy proposed in this paper is improved by 0.91% and 3.91% compared with the control strategies A and B. The results show that the braking energy recovery control strategy proposed in this paper can recover more electric energy than the other two control strategies. Figure 19c is a comparison of the energy recovered by the three control strategies. From the figure, it can be seen that the energy recovered by the control strategy proposed in this paper is about 656.90 KJ, while the energy recovered by control strategies A and B is about 603.25 KJ and 344.51 KJ. Therefore, the braking energy recovery capability of the control strategy proposed in this paper is better than the other two control strategies.

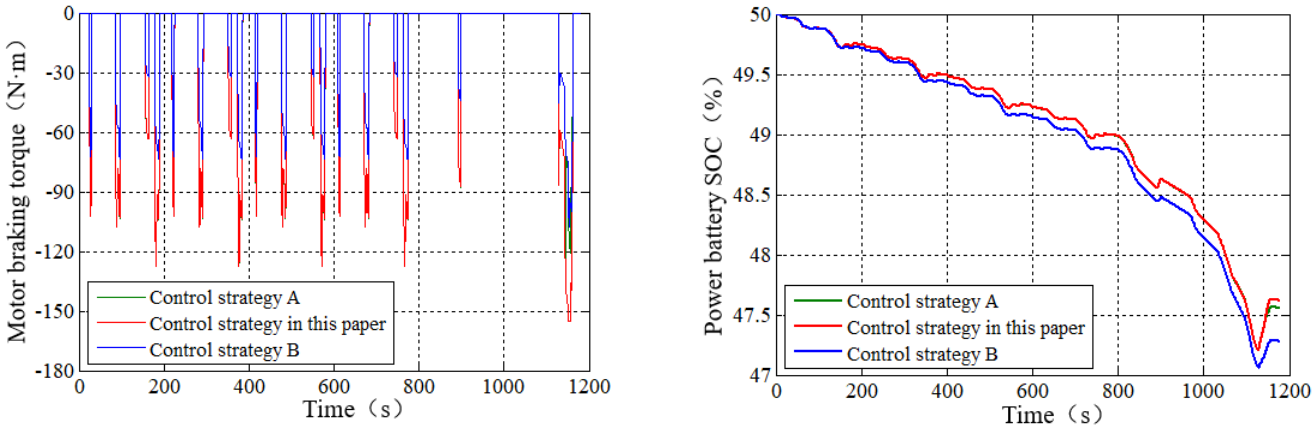

(**a**) Comparison of three control strategies for motor braking torque. (**b**) Comparison of three control strategies for power battery *SOC*.

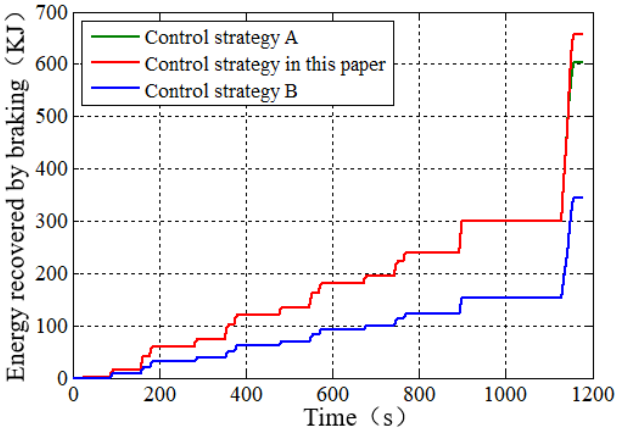

(**c**) Comparison of three control strategies for energy recovery.

Figure 19. Comparison of three control strategies in the NEDC condition.

(2) WLTC condition

Figure 20 shows the comparison of three control strategies in the WLTC condition. Among them, Figure 20a is the comparison of the motor braking torque of the three control strategies. From the figure, it is known that the motor braking torque of the control strategy proposed in this paper is better than the control strategies A and B, which proves that

the braking energy recovered by the control strategy proposed in this paper is also very impressive; Figure 20b is the comparison of the *SOC* of the power battery of the three control strategies. When the vehicle is running through the cycle condition, the *SOC* of the control strategy proposed in this paper is 44.56%, and the *SOC* of the control strategies A and B are respectively 44.45% and 43.87%. The condition of WLTC is 23.27 km, so when the vehicle drives 100 km, the battery *SOC* of the control strategy proposed in this paper is improved by 0.47% and 2.97% compared with the control strategies A and B. It can be seen directly that the energy recovered by the power battery of the control strategy proposed in this paper is higher than the other two control strategies; Figure 20c is the comparison of the energy recovered by the braking of the three control strategies. The energy recovered by the control strategy proposed in this paper is about 1420.34 KJ, while the energy recovered by the control strategies A and B is about 1324.61 KJ and 790.20 KJ. It is proved that the braking energy recovery of this control strategy is better than the other two control strategies by the amount of recovered energy.

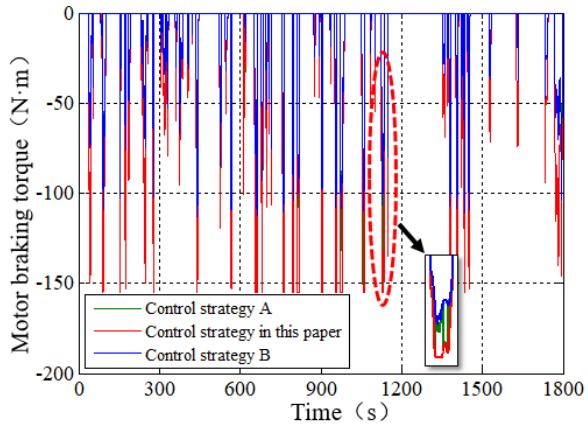

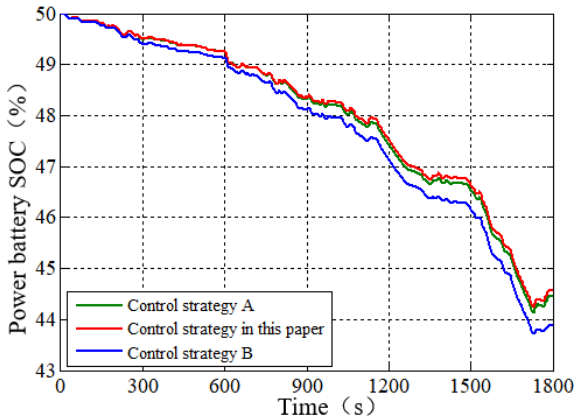

(**a**) Comparison of three control strategies for motor braking torque. (**b**) Comparison of three control strategies for power battery *SOC*.

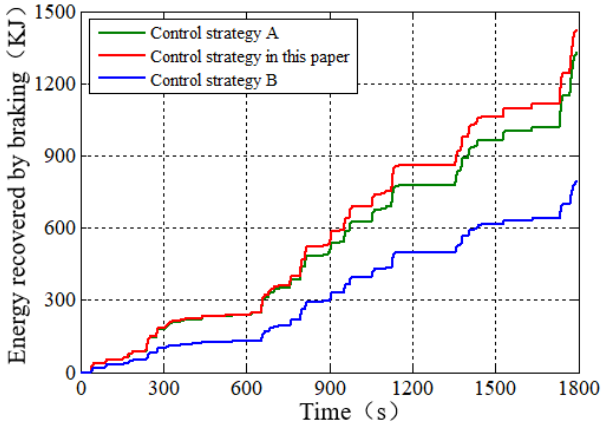

(**c**) Comparison of three control strategies for energy recovery.

Figure 20. Comparison of three control strategies in the WLTC condition.

In order to verify the effectiveness of the control strategy proposed in this paper, the Power Battery *SOC*, the effective energy recovery rate and the braking energy recovery rate are selected as the evaluation criteria. The effective energy recovery rate and the braking energy recovery rate are shown in Equations (11) and (12).

$$\eta_e = \frac{E_r}{E_b} \times 100\% \tag{11}$$

$$\eta_b = \frac{E_r}{E_v} \times 100\% \tag{12}$$

where E_r is the energy recovered by braking; E_b is the total braking energy; E_v is the energy consumption of the whole vehicle; η_e is the effective energy recovery rate in the process of vehicle braking; η_b is the braking energy recovery rate in the process of vehicle braking. The sum of η_e and η_b is calculated as shown in Table 3.

Table 3. Comparison of braking energy recovery in NEDC and WLTC conditions.

Control Strategy	Control Strategy A		Control Strategy B		Control Strategy Proposed in This Paper	
	NEDC	WLTC	NEDC	WLTC	NEDC	WLTC
Total energy consumption of vehicles (KJ)	4212.36	12,141.2	4201.19	12,043.53	4224.82	12,131.13
Total braking energy (KJ)	1640.81	3677.4	1632.72	3646.52	1676.80	3681.21
Energy recovered by braking (KJ)	603.25	1324.61	344.51	790.20	656.90	1420.34
Effective energy recovery rate (%)	14.32	10.91	8.20	6.56	15.55	11.71
Braking energy recovery rate (%)	36.76	36.02	21.10	21.67	39.18	38.58

Table 3 shows the comparison of the braking energy recovery effects of the three control strategies based on NEDC and WLTC conditions. For the control strategy proposed in this paper, in the NEDC condition, the total energy consumption of the vehicle reached 4224.82 KJ, the total braking energy produced was 1676.8 KJ and the energy recovered during braking was 656.90 KJ. Therefore, the effective braking energy recovery rate of the vehicle reached 15.55%, compared with control strategies A and B, which was increased by 1.23% and 7.35%, and the recovery rate of the braking energy reached 39.18%, which was respectively increased by 2.42% and 18.08%. In addition, in the WLTC condition, the total energy consumption of the vehicle reached 12,131.13 KJ, the total energy generated during braking was 3681.21 KJ, and the energy recovered by braking was 1420.34 KJ. Therefore, the effective recovery rate of braking energy of the vehicle reached 11.71%, which increased by 0.80% and 5.15% respectively compared with the control strategies A and B. The recovery rate of braking energy reached 38.58%, which increased by 2.56% and 16.91% respectively through comparison. To sum up, the control strategy proposed in this paper can reasonably distribute the braking force of the vehicle and effectively improve the energy recovered by the vehicle during braking.

6. Conclusions

This paper proposes a double layers multi parameters braking energy recovery control strategy. The first layer is to distribute the braking force of the front and rear axles. According to the braking strength, the braking mode is divided into three types. Within the limits of braking regulations, a corresponding front and rear axle braking force distribution control strategy is formulated for each braking mode. The second layer performs a secondary distribution of the distributed front axle braking force. By designing a fuzzy controller, which takes the speed, braking strength and the state of charge of the power battery as the input and the proportion coefficient of regenerative braking as the output, and considering the anti-drag torque of the engine, it realizes the coordinated control of the front axle electromechanical braking force.

Based on the NEDC and WLTC conditions, the control strategy in this paper is compared with control strategies A and B by simulation, and the *SOC* of power battery and the recovery efficiency of braking energy are taken as the evaluation criteria. The results show that in the NEDC condition, the battery *SOC* of the control strategy proposed in this paper is increased by 0.10% and 0.43% compared with control strategies A and B, and the braking energy recovery rate is increased by 2.42% and 18.08%, respectively. In the WLTC condition, the battery *SOC* of the control strategy proposed in this paper increased by 0.11% and 0.69%, and the braking energy recovery rate was increased by 2.56% and 16.91%, respectively.

The simulation results prove that the control strategy proposed in this paper has a great energy recovery potential and can improve vehicle energy utilization efficiency on

the premise of meeting vehicle braking requirements. In terms of theoretical research, this paper can provide a comprehensive reference for scholars in universities and automobile companies in energy recovery. In the future, the author will focus on the integration of vehicle ABS systems and regenerative braking control strategies, as well as actual vehicle tests.

Author Contributions: D.N. designed the main idea, methods and experiments, and wrote the paper. C.G. and L.G. participated in the design of the algorithm. Q.X. and S.M. put forward suggestions for revision and helped to revise the manuscript. All authors have read and agreed to the published version of the manuscript.

Funding: This work was supported by National Key Research and Development Program (2017YFB0103203).

Acknowledgments: The authors would like to thank the reviewers for their corrections and helpful suggestions.

Conflicts of Interest: The authors declare no conflict of interest.

References

1. Enang, W.; Bannister, C. Modelling and control of hybrid electric vehicles (A comprehensive review). *Renew. Sustain. Energy Rev.* **2017**, *74*, 1210–1239. [CrossRef]
2. Sharma, M.; Singh, A.N.; Yadav, R.; Jha, A.; Vanshaj, K.; Fahim, M. Regenerative Braking System. *J. Trend Sci. Res. Dev.* **2019**, *3*, 298–300. [CrossRef]
3. Xu, L.; He, X.; Shen, X. Improving Energy Recovery Rate of the Regenerative Braking System by Optimization of Influencing Factors. *Appl. Sci.* **2019**, *9*, 3807. [CrossRef]
4. Zhao, D.; Chu, L.; Xu, N.; Sun, C.; Xu, Y. Development of a Cooperative Braking System for Front-Wheel Drive Electric Vehicles. *Energies* **2018**, *11*, 378. [CrossRef]
5. Zhao, Q.; Zhang, H.; Xin, Y.; Salman, S. Research on Control Strategy of Hydraulic Regenerative Braking of Electrohydraulic Hybrid Electric Vehicles. *Math. Probl. Eng.* **2021**, *2021*, 5391351. [CrossRef]
6. He, H.; Wang, C.; Jia, H. A single-pedal regenerative braking control strategy of accelerator pedal for electric vehicles based on adaptive fuzzy control algorithm. *Energy Procedia* **2018**, *152*, 624–629.
7. Qiu, C.; Wang, G.; Meng, M.; Shen, Y. A novel control strategy of regenerative braking system for electric vehicles under safety critical driving situations. *Energy* **2018**, *149*, 329–340. [CrossRef]
8. Wu, Y.; Shu, M.; Ge, H. Research on Brake Force Distribution Control Strategy of Electric Vehicle Subtitle as needed. *Iop Conf. Ser. Mater. Sci. Eng.* **2018**, *452*, 032054. [CrossRef]
9. Xin, Y.; Zhang, T.; Zhang, H.; Zhao, Q.; Zheng, J.; Wang, C.; Pace, R.D. Fuzzy Logic Optimization of Composite Brake Control Strategy for Load-Isolated Electric Bus. *Math. Probl. Eng.* **2019**, *2019*, 9735368. [CrossRef]
10. Liu, H.; Lei, Y.; Fu, Y.; Li, X. An Optimal Slip Ratio-Based Revised Regenerative Braking Control Strategy of Range-Extended Electric Vehicle. *Energies* **2020**, *13*, 1526. [CrossRef]
11. Xu, W.; Chen, H.; Zhao, H.; Ren, B. Torque optimization control for electric vehicles with four in-wheel motors equipped with regenerative braking system. *Mechatronics* **2019**, *57*, 95–108. [CrossRef]
12. Wu, J.; Wang, X.; Li, L.; Qin, C.; Du, Y. Hierarchical control strategy with battery aging consideration for hybrid electric vehicle regenerative braking control. *Energy* **2018**, *145*, 301–312. [CrossRef]
13. Yang, Y.; He, Q.; Chen, Y.; Fu, C. Efficiency Optimization and Control Strategy of Regenerative Braking System with Dual Motor. *Energies* **2020**, *13*, 711. [CrossRef]
14. Li, S.; Yu, B.; Feng, X. Research on braking energy recovery strategy of electric vehicle based on ECE regulation and I curve. *Sci. Prog.* **2020**, *103*, 36850419877762. [CrossRef] [PubMed]
15. Xiao, B.; Lu, H.; Wang, H.; Ruan, J.; Zhang, N. Enhanced Regenerative Braking Strategies for Electric Vehicles: Dynamic Performance and Potential Analysis. *Energies* **2017**, *10*, 1875.
16. Zhou, M.; Wang, J.; Chen, Q. Research on vehicle controller and control strategy for pure electric vehicle with composite power. *Int. J. Electr. Hybrid Veh.* **2019**, *11*, 170–193. [CrossRef]
17. Ma, K.; Wang, Z.; Liu, H.; Yu, H.; Wei, C. Numerical Investigation on Fuzzy Logic Control Energy Management Strategy of Parallel Hybrid Electric Vehicle. *Energy Procedia* **2019**, *158*, 2643–2648. [CrossRef]
18. Pei, X.; Pan, H.; Chen, Z.; Guo, X.; Yang, B. Coordinated control strategy of electro-hydraulic braking for energy regeneration. *Control Eng. Pract.* **2020**, *96*, 104324. [CrossRef]
19. Sun, Y.; Wang, Y.; Zhu, R.; Geng, R.; Zhang, J.; Fan, D.; Wang, H. Study on the Control Strategy of Regenerative Braking for the Hybrid Electric Vehicle under Typical Braking Condition. *IOP Conf. Ser. Mater. Sci. Eng.* **2018**, *452*, 032092. [CrossRef]